Satellite ice extent, sea surface temperature, and atmospheric methane trends in the Barents and Kara seas

Ira Leifer[1], F. Robert Chen[2], Frank Muller Karger[2], Leonid Yurganov[3], Thomas McClimans[4]

[1] Bubbleology Research International, Inc., Solvang, CA, US. ira.leifer@bubbleology.com

[2] University of Southern Florida, US

[3] University of Maryland, Baltimore, US

[4] SINTEF Ocean, Trondheim, Norway

Supplementary Material

S1. Detailed Currents and Bathymetry

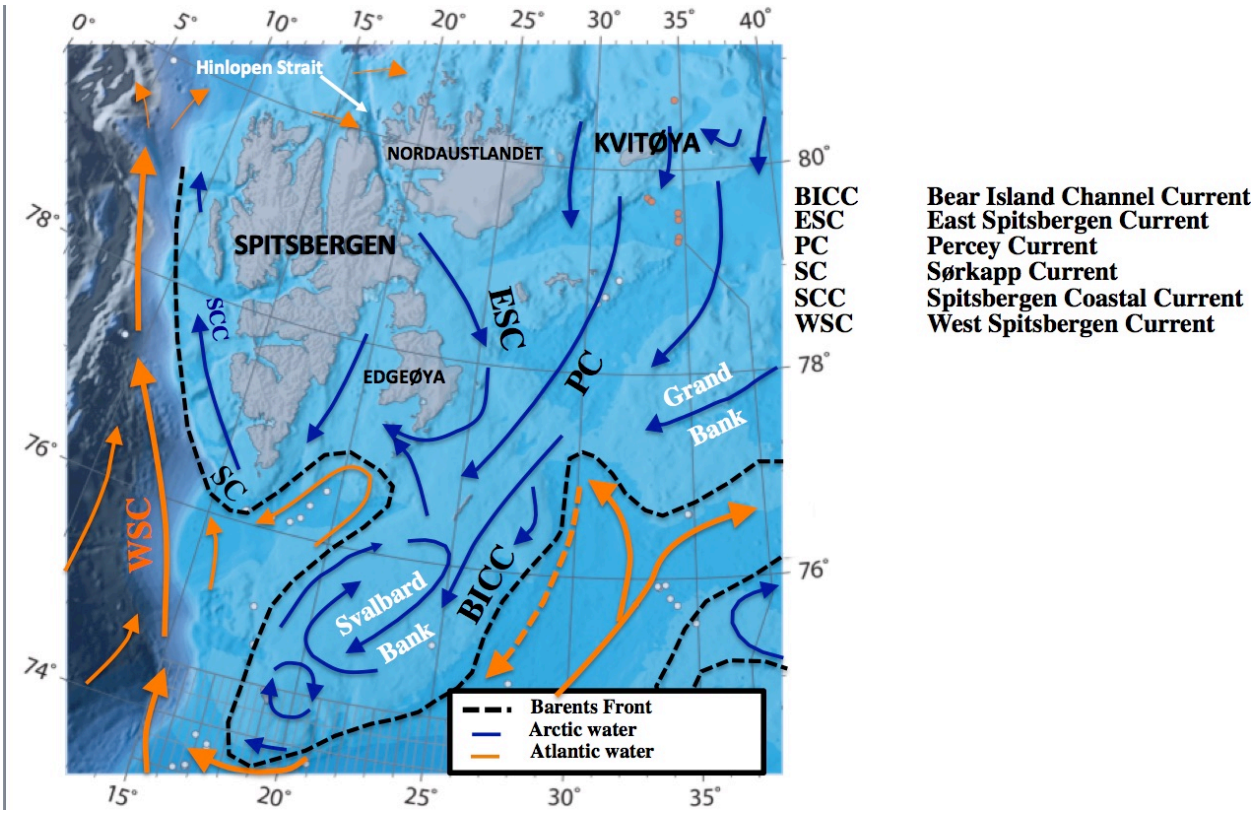

Figure S1. Bathymetry and currents around Svalbard. Bathymetry from Norwegian Petroleum Directorate (2016). Currents adapted from Stiansen et al. (2009). Dashed black line shows the Barents Front location, Dashed currents are submerged; blue - cold, yellow - warm.

Currents and flows around Svalbard Archipelago are complex (**Supp. Fig. S1**), dominated by the West Spitsbergen Current (WSC), which is the northerly fork of the Norwegian Atlantic Current (NAC), and flows northwards off the west coast of Spitsbergen. The cold, Percy Current (PC) flows southwest off the eastern shores of the Svalbard Archipelago. The cold East Spitsbergen Current (ESC) flows through the Hinlopen Strait and then joins the PC to flow around the south cape of Spitsbergen as the Sørkapp Current (SC), following the coast northwards as the Spitsbergen Coastal Current (SCC) (Svendsen et al., 2002). The cold SCC flows inshore of the WSC, and flows up Svalbard's western coast, inshore and shallower than the warm, Atlantic WSC. The interface between these two currents off west Spitsbergen forms a part of the Barents Front. Thus, coastal waters offshore West Spitsbergen are of Arctic Ocean origin, whereas further offshore lies Barents Sea water (origin Atlantic Ocean).

The location of the Barents Sea Polar Front (Oziel et al., 2016) is semi-permanent and controlled by seabed topography (**Fig. S1**), particularly the Svalbard Bank and Grand Bank and the trough to the southwest of Svalbard.

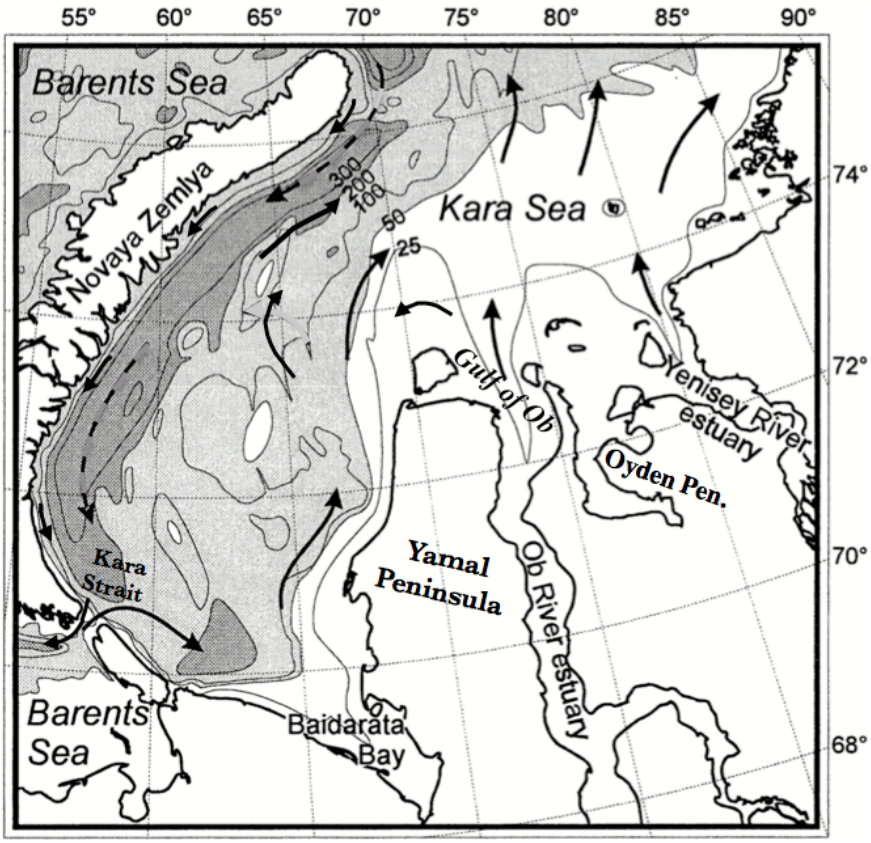

Figure S2. Bathymetry and currents for the Kara Sea. Adapted from Polyak et al. (2002) and McClimans et al. (2000). Dashed line indicates subsurface flow.

The Ob and Yenisei Rivers outflow 350 and 650 km^3 yr^{-1}, respectively (Stedmon et al., 2011), into the Kara Sea, which is largely extremely shallow causing it to be mostly brackish. Combined with inflow from the Barents Sea, currents for half of the Kara Sea are largely northwards. The exception is the more than 300 m deep Novaya Zemlya Trough where water enters from the north Barents Sea and flows below the brackish surface waters.

Cold Arctic waters flow along the eastern shore of Novaya Zemlya is the narrow, weak Novaya Zemlya Coastal Current (NZCC) and as a deep submerged flow through the Novaya Zemlya Trough. The NZCC exits through the same Kara Strait that Barents Sea water inflows. This, in combination with the rising shallow seabed, causes the Kara Strait to be a site of likely strong mixing. Brackish riverine outflow across the Kara Sea compresses the cold southwards flow east of Novaya Zemlya both from the east and from above.

The Ob and Yenisei Rivers transport significant sediment, underlying the shallowness of the Kara Sea, with extensive proven and proposed, petroleum hydrocarbon reservoirs underlying the southeast Kara Sea (Rekacewicz, 2005). Given the Kara Sea's shallowness, methane (CH_4) seep seabed bubbles can mostly transfer their gas directly to the atmosphere (Leifer et al., 2017; Leifer and Patro, 2002) and indirectly from wind mixing (Wanninkhof and McGillis, 1999), and also from storm sparging (Boitsov et al., 2012; Shakhova et al., 2013), which in the Arctic can extend to 100-200 m depth, i.e., most of the Kara Sea.

S.2. Barents Sea *in situ* data

Carbon dioxide and CH_4 *in situ* data were collected by a Cavity Enhanced Absorption Spectrometer (CEAS), Greenhouse Gas Analyzer (Los Gatos, Research, Mountainview, CA) onboard the *R/V Akademik Fyodorov* during the Nansen and Amundsen Basins Observational System (NABOS) expedition in fall 2013. The *R/V Akademik Fyodorov* is 141 m long with a 25 m beam and an 8 m draught. The *R/V Akademik Fyodorov* departed Kirkenes,

Norway on 21 Aug. 2013, returning to Kirkenes on 23 Sept. 2013. Analyzer performance information also was recorded for data quality review. Instrument precision was ~1 ppb with a 10 s response time and a 117 s mean layback time. Samples were collected from above the main superstructure, approximately 25 m above the sea surface (**Fig. S3a**), Calibration was daily and used a cylinder standard provided by the Norwegian Air Research Institute (NILU).

The main potential source of ship pollution could be the diesel engine exhaust; however, it appears that the *Akademik Fyodorov*'s engine is not a source of CH_4, with atmospheric CH_4 partially oxidized by the engine leading to exhaust gas having depressed CH_4 compared to ambient air. Data analyzed herein were during steaming transit across the Barents Sea at 26 km hr^{-1}, for which other potential vessel sources, such as the sewage storage venting are not relevant.

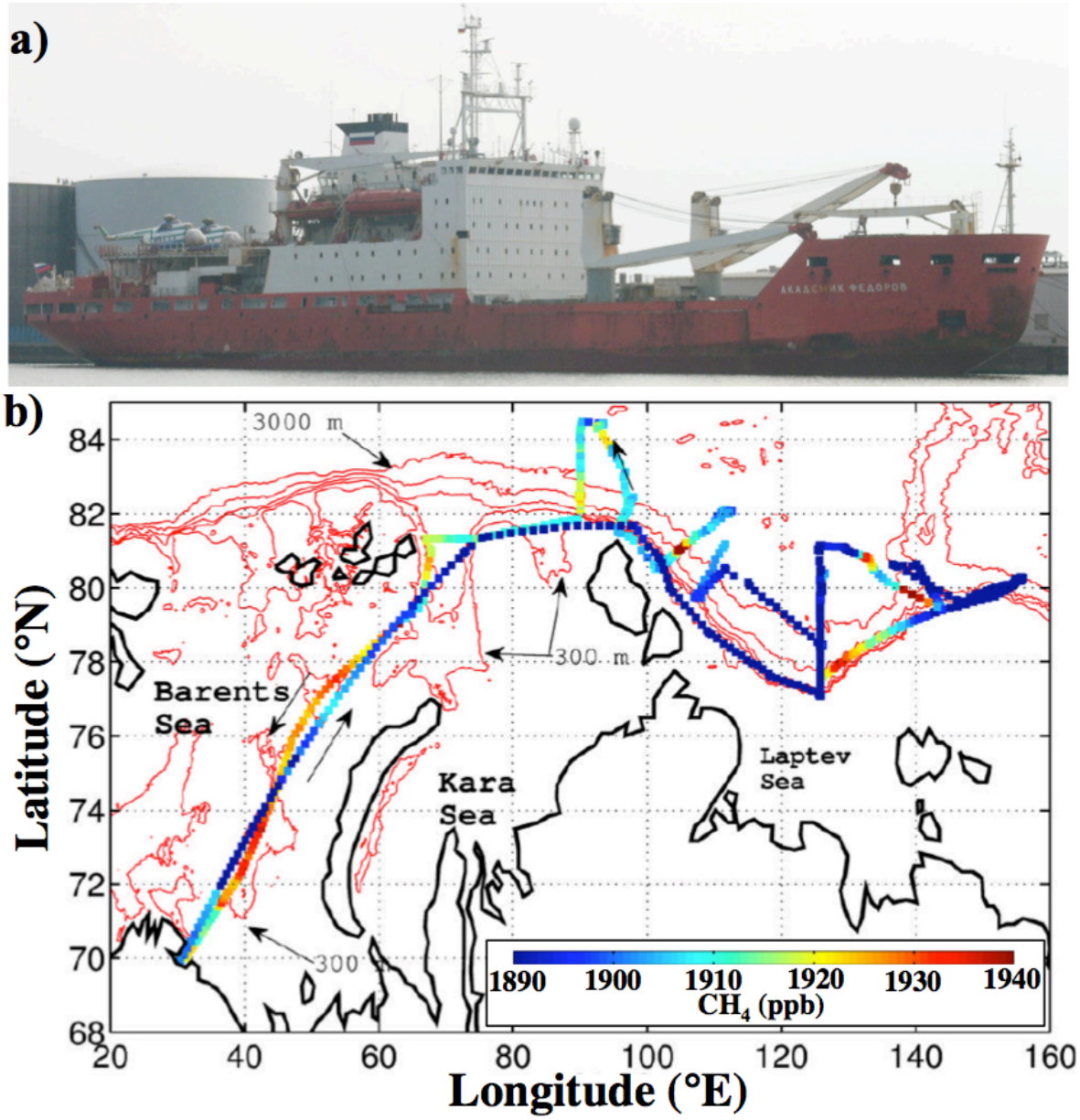

Figure S3. a) Photo of the *R/V Akademic Fyodorov*. **b)** Hourly averaged methane (CH_4) from NABOS expedition. Data key on figure.

The month-long data set showed a significant difference between the northwards and southwards transits of the Barents Sea, which were separated by approximately one month. Most of the values in the Laptev Sea were low, although there were several localized areas of enhanced CH_4.

NABOS values were compared with satellite-retrieved column CH_4 from Infrared Atmospheric Sounder Interferometer (IASI) for 21-24 Aug. 2013 for the 21 Aug. 2013 northwards transit and for 17-22 Sept. 2013 for the 23 Sept. 2013 southwards transit. Agreement between IASI lower tropospheric CH_4 and *in situ* CH_4 for the northwards transit were good, within ~10 ppb. Agreement was much poorer for the southwards transit.

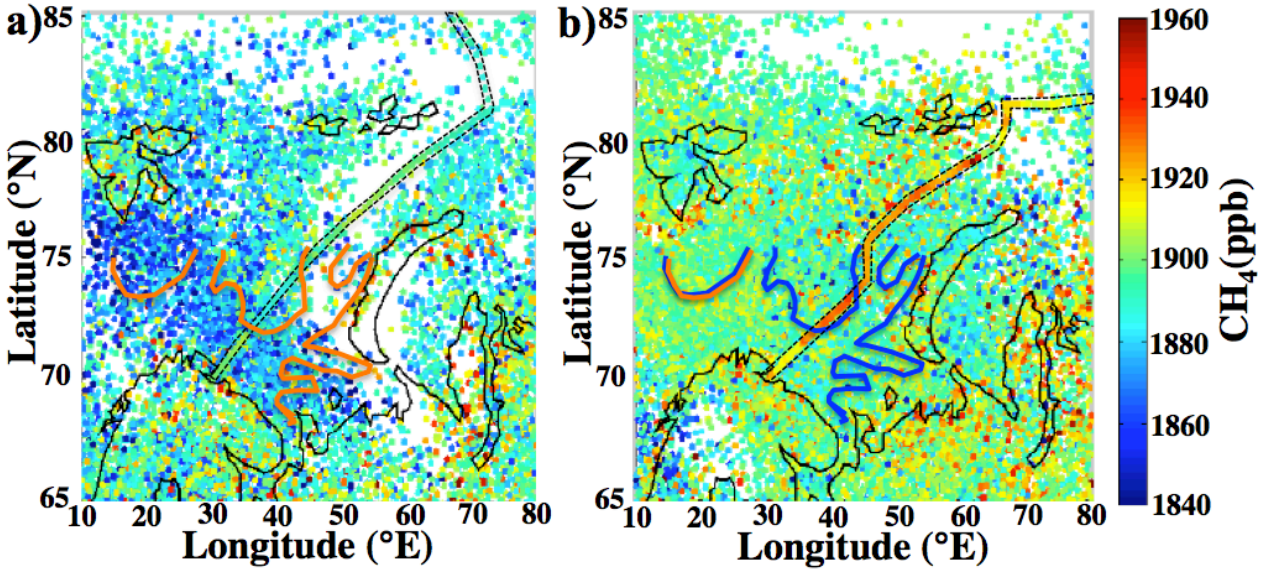

Figure S4. a) IASI retrieved 0-4 km methane (CH_4) for 21-24 Aug. 2013 and hourly CH_4 from the NABOS cruise (outlined in dashed line black). Also shown is the Murman Coastal Current's edges, from Alexeev et al. (2018) and **b)** for 17-22 Sept. 2013. Data key on figure.

S.3. Focus Areas

Supp. Table S1. Focused study area coordinates

Area	Up Left	Up Right	Lower Left	Lower Right
1	79° 16'6.91" N 60° 48'53.42" E	78° 32'12.26" N 62° 49'54.69" E	78° 55'5.27" N 57° 43'42.58" E	78° 12'27.81" N 59° 52'32.46" E
2	78° 38'25.09" N 55° 34'48.90" E	77° 56'45.71" N 57° 48'15.36" E	78° 14'20.21" N 52° 49'55.73" E	77° 34'0.24" N 55° 8'13.34" E
3	79° 10'4.24" N 41° 13'50.40" E	78° 36'13.19" N 44° 21'38.03" E	78° 38'35.38" N 38° 57'26.67" E	78° 6'12.61" N 42° 3'28.98" E
4	79°38'46.04" N 5° 40'51.21" E	79° 31'53.40" N 10° 11'25.49" E	78° 57'49.65" N 5° 19'46.85" E	78° 51'21.95" N 9° 34'7.45" E
5	78° 8'40.32" N 0° 36'30.89" E	78° 6'24.41" N 4° 35'53.20" E	77° 27'29.19" N 0° 34'31.46" E	77° 25'20.57" N 4° 20'54.29" E
6	76° 11'22.21" N 1° 16'10.96" E	76° 8'46.20" N 4° 41'44.27" E	75° 30'6.27" N 1° 12'35.25" E	75° 27'37.48" N 4° 28'29.63" E
7	74° 48'24.40" N 12° 40'7.63" E	74° 36'9.07" N 15° 40'42.21" E	74° 8'1.53" N 12° 7'35.64" E	73° 56'16.20" N 15° 1'6.10" E
8	73° 34'52.37" N 33° 48'43.77" E	73° 6'7.85" N 36° 8'55.31" E	73° 0'12.51" N 32° 31'37.62" E	72° 32'23.29" N 34° 49'20.56" E
9	72° 46'29.04" N 48° 59'20.20" E	72° 8'6.72" N 50° 44'6.03" E	72° 18'49.49" N 47° 18'49.40" E	71° 41'23.16" N 49° 4'27.27" E

10	74° 48’6.77” N 38° 38’57.13” Ë	74° 16’3.18” N 41° 0’24.96” E	74° 15’28.49” N 37° 5’34.21” E	73° 44’27.53” N 39° 25’24.39” E

S.4. Summer month sea surface temperature and methane trends

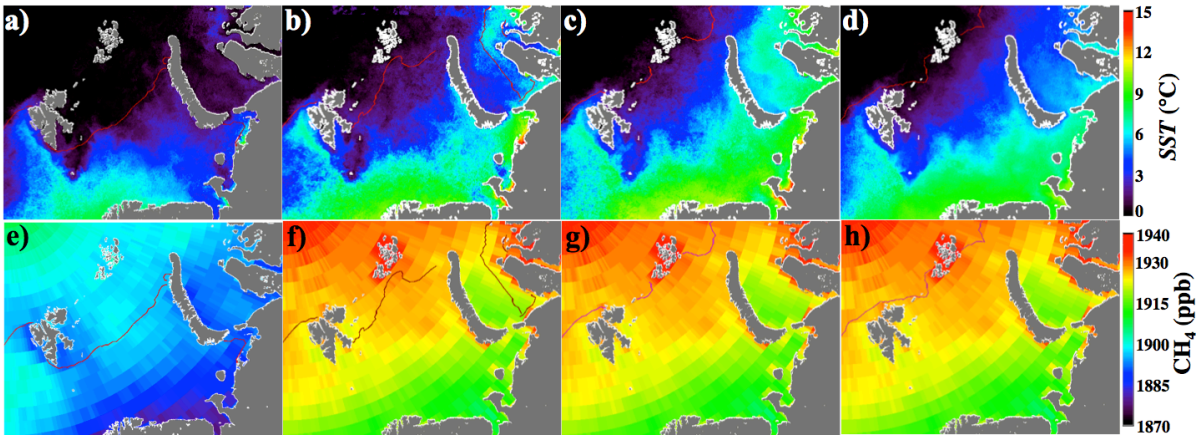

Figure S5. Mean values for 2003 to 2015 of sea surface temperature (*SST*) for **a**) June, **b**) July, **c**) August, and **d**) September. Mean methane (CH_4) concentration for **e**) June, **f**) July, **g**) August, and **h**) September. Median ice edge for same period is shown. Years with reduced ice extent contribute to values of *SST* north of the ice edge. Data keys on figure.

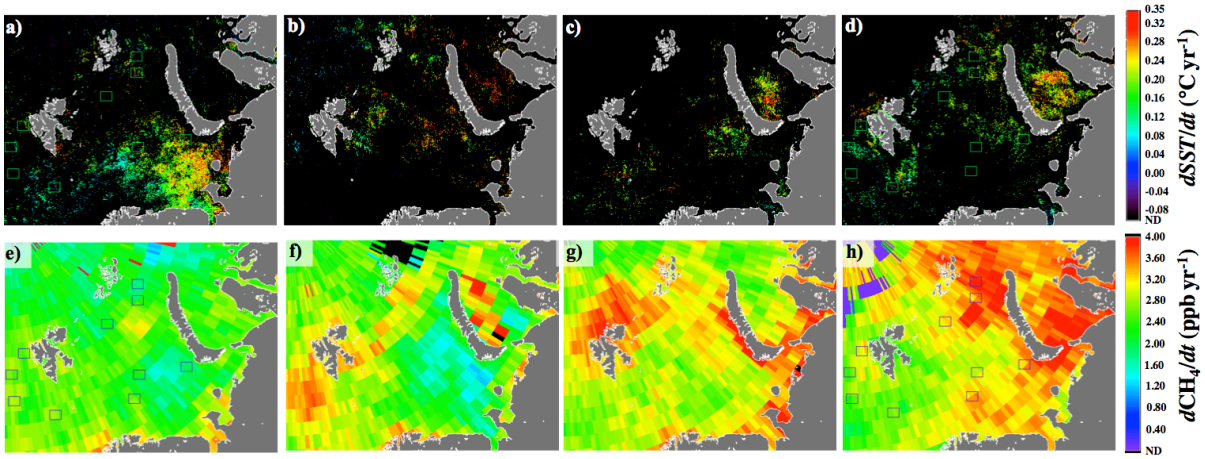

Figure S6. Linear trends for 2003 to 2015 of sea surface temperature ($dSST/dt$) for **a**) June, **b**) July, **c**) August, and **d**) September. Methane concentration trend (dCH_4/dt) for **e**) June, **f**) July, **g**) August, and **h**) September. ND – not detectable, i.e., failed statistical test. Blue, black dashed lines shows 100 and 50 m contour, respectively. Data key on figure.

S.5. Barents and Kara Seas Oil and Gas Reservoirs

The Barents and Kara seas contain significant and extensive oil and gas reserves, which in the case of the Russian Kanin Peninsula extend onshore where they are produced and transported by pipeline (**Fig. S7**). Additional extensive proven hydrocarbon resources are found in the shallow southeast Kara Sea. It is likely, given the relationship between major river outflows and hydrocarbon reserves globally (e.g., the Mississippi, the Amazon, the Congo, the Nile) that similar reserves underlie the shallow northeastern Kara Sea.

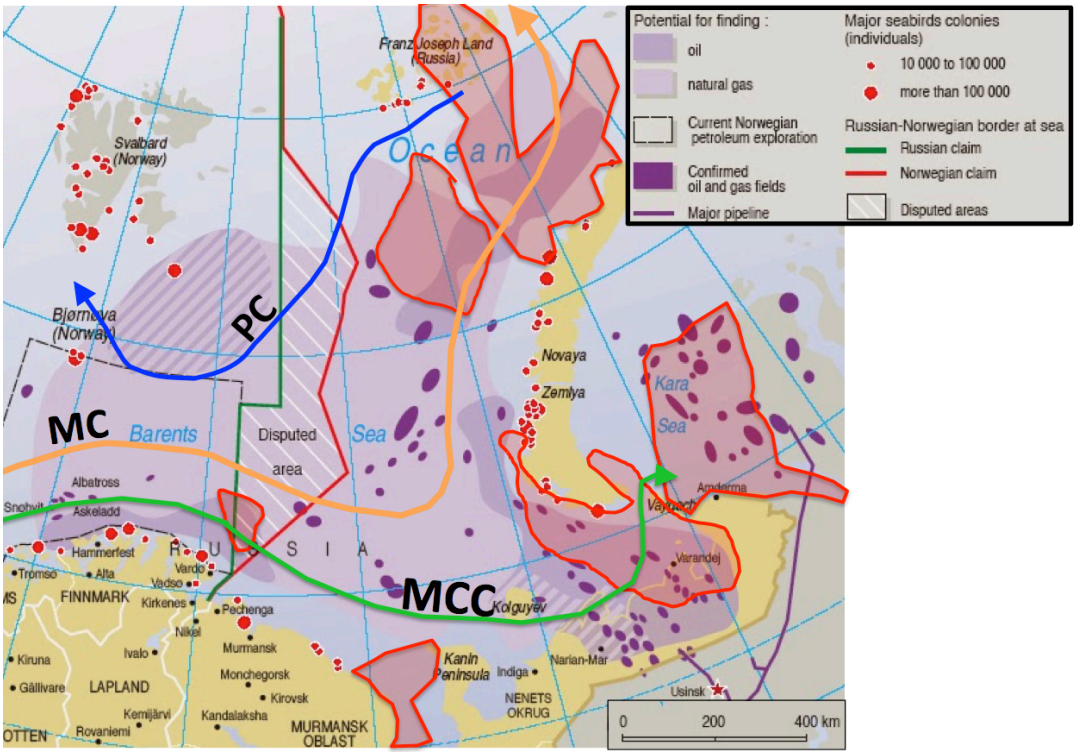

Figure S7. Barents Sea location of oil and gas fields and potential fields, and pipelines. Also shown are the approximately locations of the major Barents Sea currents – the Murman Current (MC), Murman Coastal Current (MCC) and the Percey Current (PC). Outlined in red are areas where $dCH_4/dt > 3$ ppb yr^{-1} from **Fig. 11**. Adapted from Rekacewicz (2005).

S.6. Arctic Methane Movie

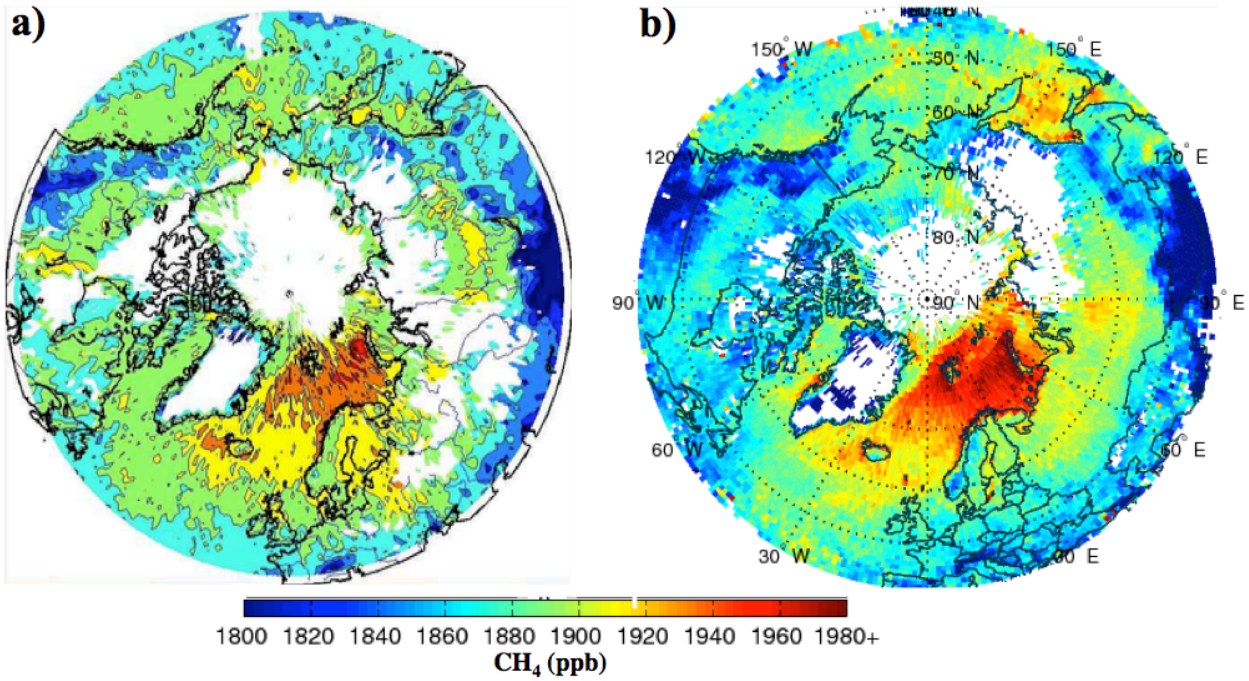

Figure S8. IASI Arctic methane (CH_4) for the lower 4 km for a) March 2012 and b) March 2018.

A movie of Arctic CH_4 from 2012 every 5 days shows a range of variations on a range of different spatial and temporal scales. Strong enhancements are observed that persist in regions for a few days – most likely related to synoptic system flushing in fall to spring. The seasonal variation is easily observed, with highest values often in November and December. In late winter and early spring, large CH_4 anomalies are observed in some years at the ice edge.

References

Alexeev, A. P., Semenov, A. V., Borovkov, V. A., Tereshchenko, V. V., and Shleinik, V. N.: http://www.pinro.ru/labs/hid/kolsec1_e.htm, last access: 25 March 2018 2018.

Boitsov, V. D., Karsakov, A. L., and Trofimov, A. G.: Atlantic water temperature and climate in the Barents Sea, 2000–2009, ICES J. Mar. Sci., 69, 833-840, 2012.

Leifer, I., Chernykh, D., Shakhova, N., and Semiletov, I.: Sonar gas flux estimation by bubble insonification: Application to methane bubble flux from seep areas in the outer Laptev Sea, The Cryosphere, 11, 1333-1350, 2017.

Leifer, I. and Patro, R.: The bubble mechanism for methane transport from the shallow sea bed to the surface: A review and sensitivity study, Continental Shelf Research, 22, 2409-2428, 2002.

McClimans, T. A., Johnson, D. R., Krosshavn, M., King, S. E., Carroll, J., and Grenness, Ø.: Transport processes in the Kara Sea, J. Geophys. Res.: Oceans, 105, 14121-14139, 2000.

Norwegian Petroleum Directorate: Resource Report, Norwegian Petroleum Directorate,, Stavanger, Norway, 56 pp., 2016.

Oziel, L., Sirven, J., and Gascard, J. C.: The Barents Sea frontal zones and water masses variability (1980–2011), Ocean Sci., 12, 169-184, 2016.

Polyak, L., Korsun, S., Febo, L. A., Stanovoy, V., Khusid, T., Hald, M., Paulsen, B. E., and Lubinski, D. J.: Benthic foraminiferal assemblages from the Souterhn Kara Sea - A river-influenced Arctic marine environment, The J. Foraminiferal Res., 32, 252-273, 2002.

Rekacewicz, P.: https://www.grida.no/resources/7482) last access: January 2018 2018.

Shakhova, N., Semiletov Igor P., Leifer, I., Sergienko, V., Salyuk, A., Kosmach, D., Chernikh, D., Stubbs, C., Nicolsky, D., Tumskoy, V., Alexeev, V., and Gustafsson, O.: Ebullition and storm-induced methane release from the East Siberian Arctic Shelf, Nature Geosci., 7, 64-70, 2013.

Stedmon, C. A., Amon, R. M. W., Rinehart, A. J., and Walker, S. A.: The supply and characteristics of colored dissolved organic matter (CDOM) in the Arctic Ocean: Pan Arctic trends and differences, Mar. Chem., 124, 108-118, 2011.

Stiansen, J. E., Korneev, O., Titov, O., Arneberg, P., Filin, A., Hansen, J. R., Høines, Å., and Marasaev, S.: Joint Norwegian-Russian environmental status 2008. Report on the Barents Sea Ecosystem. Part II – Complete report, Norwegian Marine Data Center (NMDC)1502-8828, 375 pp., 2009.

Svendsen, H., Beszczynska-Møller, A., Hagen, J. O., Lefauconnier, B., Tverberg, V., Gerland, S., Ørbøk, J. B., Bischof, K., Papucci, C., Zajaczkowski, M., Azzolini, R., Bruland, O., Wiencke, C., Winther, J. G., and Dallmann, W.: The physical environment of Kongsfjorden–Krossfjorden, an Arctic fjord system in Svalbard, Polar Res., 21, 133-166, 2002.

Wanninkhof, R. and McGillis, W. R.: A cubic relationship between air-sea CO_2 exchange and wind speed, Geophys. Res. Lett., 26, 1889-1892, 1999.